

# Power gain exhibited by motile mechanosensory neurons in *Drosophila* ears

M. C. Göpfert\*<sup>†</sup>, A. D. L. Humphris<sup>‡</sup>, J. T. Albert\*, D. Robert<sup>§</sup>, and O. Hendrich\*

\*Volkswagen Foundation Research Group, Institute of Zoology, University of Cologne, Weyertal 119, D-50923 Cologne, Germany; <sup>†</sup>H. H. Wills Physics Laboratory, University of Bristol, Tyndall Avenue, Bristol BS8 1TL, United Kingdom; and <sup>§</sup>School of Biological Sciences, University of Bristol, Woodland Road, Bristol BS8 1UG, United Kingdom

Edited by A. James Hudspeth, The Rockefeller University, New York, NY, and approved November 27, 2004 (received for review August 5, 2004)

In insects and vertebrates alike, hearing is assisted by the motility of mechanosensory cells. Much like pushing a swing augments its swing, this cellular motility is thought to actively augment vibrations inside the ear, thus amplifying the ear's mechanical input. Power gain is the hallmark of such active amplification, yet whether and how much energy motile mechanosensory cells contribute within intact auditory systems has remained uncertain. Here, we assess the mechanical energy provided by motile mechanosensory neurons in the antennal hearing organs of *Drosophila melanogaster* by analyzing the fluctuations of the sound receiver to which these neurons connect. By using dead WT flies and live mutants (*tilB<sup>2</sup>*, *btv<sup>SP1</sup>*, and *nompA<sup>2</sup>*) with defective neurons as a background, we show that the intact, motile neurons do exhibit power gain. In WT flies, the neurons lift the receiver's mean total energy by 19 zJ, which corresponds to 4.6 times the energy of the receiver's Brownian motion. Larger energy contributions (200 zJ) associate with self-sustained oscillations, suggesting that the neurons adjust their energy expenditure to optimize the receiver's sensitivity to sound. We conclude that motile mechanosensory cells provide active amplification; in *Drosophila*, mechanical energy contributed by these cells boosts the vibrations that enter the ear.

cochlear amplifier | hearing | auditory mechanics | cell motility | hair cell

The cochlear amplifier is the dominant unifying concept in cochlear mechanics (1). The concept assumes that the cochlea is endowed with a biological energy source that amplifies the ear's input by pumping mechanical energy into the vibrations inside the ear (1–6). The validity of the concept is supported by the mechanics of the cochlea and its mechanosensory cells. Hair cells, the cochlear mechanosensory cells, provide a source of mechanical energy. In addition to transducing mechanical vibrations into electrical responses, some hair cells are equipped with molecular motors that convert metabolic or electrical energy into mechanical energy, resulting in active movements of the cells (1, 3–7). These cellular movements, in turn, exert positive feedback on the cochlear mechanics. By nonlinearly undamping the cochlear resonances as the stimulus intensity declines, this feedback selectively improves the ear's sensitivity to small vibrations induced by faint sound (1, 3–6). Notably, this hair cell-based feedback occasionally becomes unstable, leading to self-sustained feedback oscillations within the cochlear duct. Such self-sustained feedback oscillations may account for the ear's ability to generate spontaneous otoacoustic emissions, i.e., to spontaneously emit sound (8, 9).

Collectively, the hair cells' motility, the cochlea's nonlinearity, and the ear's spontaneous otoacoustic emissions document the presence of hair cell-based mechanical feedback inside the cochlear duct. Yet, whether this feedback brings about power gain by expending biological energy, as assumed by the concept of the cochlear amplifier, remains uncertain (1). Intuitively, the mere occurrence of large-amplitude spontaneous otoacoustic emissions suggests that such a power gain exists, a notion that is supported by the temporal and spectral properties of these emissions (10) and the propagation of power fluxes within the

cochlear duct (11). Yet, in strict terms, testing the existence of power gain must be based on violations of a fundamental principle of thermodynamics, the equipartition theorem, or the fluctuation-dissipation theorem (12, 13). Such violations have been demonstrated for isolated hair cells (13, 14), yet their identification in intact auditory systems has been hampered by the structural and functional complexity of the cochlea, along with its limited accessibility to mechanical examination.

The antennal hearing organs of *Drosophila melanogaster* provide an attractive model system for evaluating whether motile mechanosensory cells contribute mechanical energy within an intact ear. In the fly, the distal part of the antenna with its lateral, feathery arista (Fig. 1A *Inset*) vibrates in response to acoustic stimulation and, analogous to our eardrum, mediates the reception of sound (15, 16). The fly's antennal sound receiver is proximally suspended by an antennal joint and several hundred mechanosensory neurons (15, 16). These neurons are motile and nonlinearly modulate the receiver's tuning, shifting down its natural frequency from  $\approx 800$  to 200 Hz as the stimulus declines (17). The intimate connection between motile mechanosensory cells and an external, experimentally accessible sound receiver means that, in *Drosophila*, the mechanics of the receiver can be used to noninvasively assess the energy provided by the motile sensory cells within the ear. Exploiting this experimental advantage and profiting from the availability of mechanosensory mutants with defective, immotile neurons (17–19), we have tested for possible violations of the equipartition theorem in the ear of the fly. The approach we present is based on two premises, interindividual comparability and constancy of the mass, both of which are validated by experimental results. Violations of the equipartition theorem show that the auditory mechanosensory cells of *Drosophila* expend energy to power vibrations, as is expected for the cochlear amplifier in vertebrate ears.

## Materials and Methods

**Flies.** Flies were raised on a standard commercial medium at 22–25°C. Oregon-R was used as the WT stock. The *tilB<sup>2</sup>*, *nompA<sup>2</sup>*, and *btv<sup>SP1</sup>* mechanosensory mutants have been described (20, 21). As in dead flies, their antennal receivers respond linearly to sound (17). *tilB<sup>2</sup>* mutants were obtained by selecting hemizygous males from the balanced stock *yw tilB<sup>2</sup>/FM4*, *nompA<sup>2</sup>* mutants were selected from the balanced stock *w; cn bw nompA<sup>2</sup>/Cy P{Ubi-GFP}*, and *btv<sup>SP1</sup>* mutants were kept as homozygous stock *w; btv<sup>SP1</sup> P{FRT, neo}40A P{FRT, w<sup>+mc</sup>}G13*. The respective genetic backgrounds, *y w* (for *tilB<sup>2</sup>*), *cn bw* (for *nompA<sup>2</sup>*), and *w; P{FRT, neo}40A P{FRT, w<sup>+mc</sup>}G13* (for *btv<sup>SP1</sup>*), were used as controls.

**Mechanical Measurements.** All measurements were carried out on a TMC (Peabody, MA) 78-443-12 vibration isolation table positioned in the center of an anechoic chamber (dimensions: 4.5 × 2.25 ×

This paper was submitted directly (Track II) to the PNAS office.

<sup>†</sup>To whom correspondence should be addressed. E-mail: m.gopfert@uni-koeln.de.

© 2004 by The National Academy of Sciences of the USA

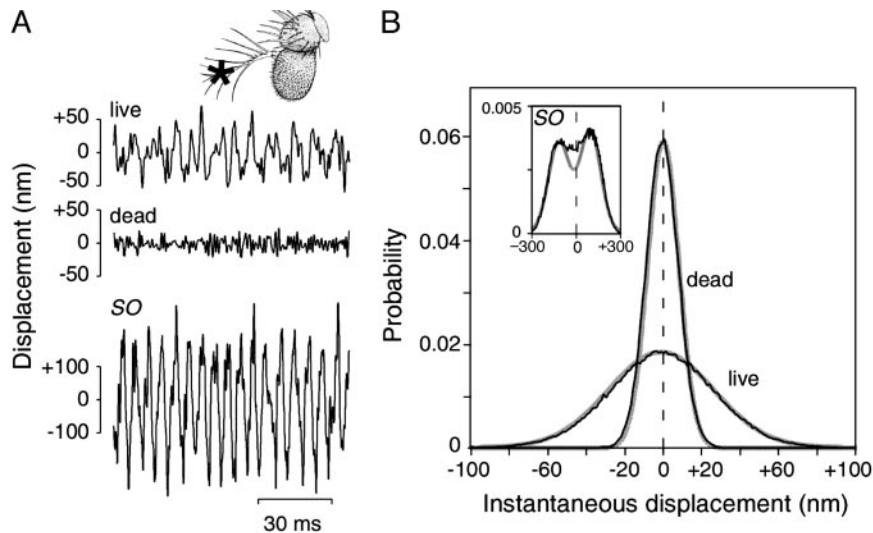


**Fig. 1.** Mechanical fluctuations of the antennal receiver. (A) Time traces of the displacement of a WT receiver measured *in vivo*, postmortem, and during self-sustained oscillations (SO) induced by thoracic injection of DMSO. Note the different scale at the bottom. (Inset) Fly antenna depicting the measurement site (\*). [Drawing reproduced with permission from ref. 34 (Copyright 2003, The FlyBase Consortium).] (B) Probability distributions of the receiver's instantaneous displacement *in vivo* and postmortem, and during SO (Inset). Measured distributions (black traces) are fitted with a Gaussian or the sum of two Gaussians (Inset, ghost traces). The distributions (160 bins) are based on 15.3-s time traces and a total of 196,530 positions each.

2 m). The animals were affixed ventrum down on top of a holder, with their heads, mouth parts, wings, halteres, and legs being stabilized by wax to minimize movements. Mechanical vibrations of the antennal receiver were measured by using a computer-controlled Polytec (Waldbronn, Germany) PSV-300 scanning laser Doppler vibrometer with an OFV-056 scanning head and an OFV-3001-S beam controller. Per animal, one receiver was examined. The vibrations of the receiver were measured near the tip of the arista, where the arista gives rise to its outermost lateral branches (Fig. 1A Inset). This measurement site was chosen for two reasons. First, the site maximally reflects the laser beam, facilitating sensitive vibration measurements in nonloading conditions. Second, the site is easily identified by using the branches of the arista as landmarks, allowing us to reproducibly position the laser beam on the receiver. Remaining interindividual variations of the measurement positions were randomized by analyzing the receivers of 20 animals per strain, with animals of different strains being examined in a random order.

For analysis, the laser signal was conditioned by anti-aliasing filters and sampled at a rate of 12 kHz by using an Analogic-Fast-16 AD board (Analogic, Peabody, MA). Fast Fourier transforms were determined on the basis of 80–100 averaged time windows (rectangular windowing function, 650-ms window length). All values are expressed as means  $\pm$  one SD.

**Receiver Fluctuations.** Mechanical fluctuations of the antennal receiver were measured in the absence of external stimulation. Frequency spectra of the receiver's Fourier-transformed velocity amplitudes,  $\dot{X}(\omega)$ , were determined for frequencies,  $f$ , between 100 and 1,500 Hz. The velocity amplitudes were converted into displacement amplitudes,  $X(\omega) = \dot{X}(\omega)/\omega$  with  $\omega = 2\pi f$ , and subsequently squared, yielding the power spectral density,  $X^2(\omega)$ , of the receiver's displacement (Fig. 2).

To mechanically characterize the receiver's fluctuations, the power spectrum was modeled by fitting the function of a simple forced damped harmonic oscillator to the receiver's resonance (Fig. 2). The fit function is described by

$$X^2(\omega) = \frac{F_0^2/m^2}{(\omega_0^2 - \omega^2)^2 + \left(\omega \frac{\omega_0}{Q}\right)^2}, \quad [1]$$

in which  $F_0$  is the strength of the external force acting on the oscillator,  $m$  is the oscillator's apparent mass,  $\omega_0$  is the natural angular frequency, and  $Q$  is the quality factor. The quality factor is defined by  $Q = m\omega_0/\gamma$ , with  $\gamma$  representing the damping constant. The natural angular frequency, in turn, refers to the undamped system,  $\omega_0 = \sqrt{K_S/m}$ , whereby  $K_S$  denotes the oscillator's spring constant. The corresponding angular frequency of the damped system,  $\omega_d$ , can be deduced as  $\omega_d = \sqrt{\omega_0^2 - \gamma^2/4m^2}$ . The shape of the fit function (Eq. 1) is described by two free parameters,  $\omega_0$  and  $Q$ , whereas the amplitude offset of the function depends on the ratio  $F_0/m$ . Integrating the function for frequencies between zero and infinity yields the fluctuation power, i.e., the mean-square displacement,  $\langle X^2 \rangle$ , of the receiver's fluctuations,

$$\langle X^2 \rangle = \int_0^\infty X^2(\omega) d\omega. \quad [2]$$

The model (Eq. 1) closely described the fluctuations of the antennal receivers of dead and live flies (Fig. 2A and F), confirming that these fluctuations themselves have a Lorentzian line shape. Background noise, which might add power to the fluctuations, is unlikely to display a resonance at the receiver's natural frequency. Hence, fitting the model to the receiver's resonance helps to isolate the receiver's fluctuations from unrelated noise.

## Results

In the absence of external stimulation, the mechanical fluctuations of the antennal receivers of intact WT flies displayed irregular, noisy twitches (Fig. 1A). These spontaneous twitches built up into large-amplitude, self-sustained oscillations when the physiological condition of the animal deteriorated [e.g., after thoracic injection of DMSO (17, 22)] and disappeared with the animal's death (Fig. 1A). Postmortem, the probability distribution of the receiver's displacement was symmetric around zero and closely followed a Gaussian, as is expected for the passive, thermal fluctuations of a harmonic oscillator (Fig. 1A). A comparable distribution characterized the fluctuations of the receiver in intact live flies, yet the distribution was broader,

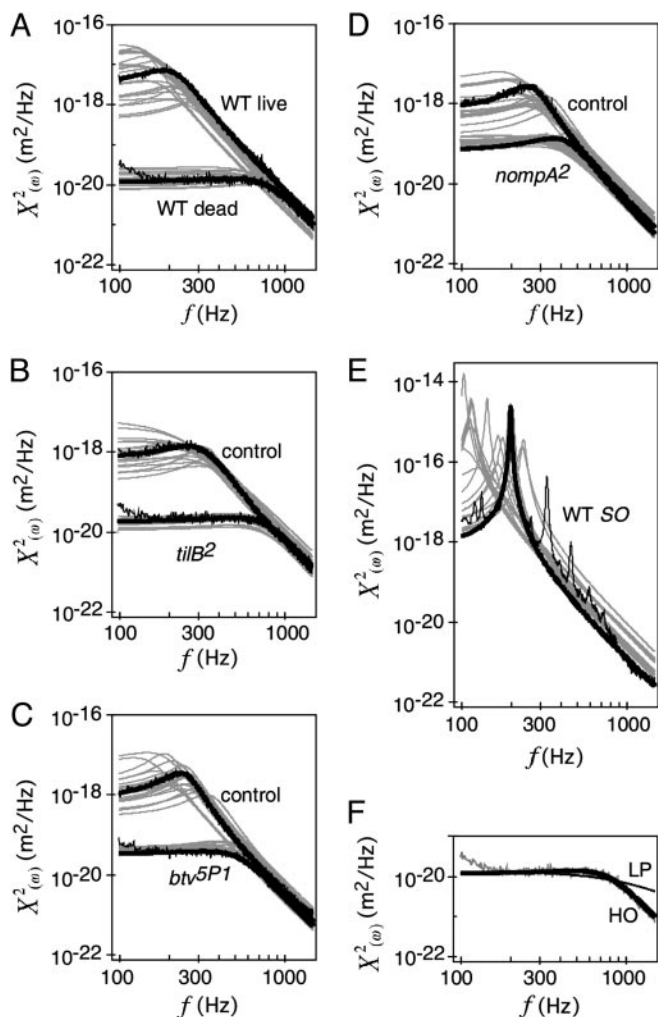


**Fig. 2.** Frequency characteristics of receiver fluctuations. (A–E) Power spectra of the receiver’s displacement in dead and live WT flies (A), live mechanosensory mutants and controls (B–D), and WT flies displaying self-sustained receiver oscillations (SO) after injection of DMSO (E) (log-log plots). Black traces in A–D highlight the measured spectrum and the fitted harmonic oscillator function for one receiver per strain, and fit functions for other receivers are depicted in gray.  $n = 20$  animals per strain. (F) Measured spectrum of the receiver of a dead fly (gray) fitted with the function of both a harmonic oscillator (HO, thick black line) and a low pass filter (LP, thin black line). The two functions are distinguished by their high-frequency roll-offs [–24 dB/octave (HO) vs. –12 dB/octave (LP)]. The near-perfect fit of the HO function, in line with the poor fit of the LP function, identifies the receiver as a spring-mass system with high-frequency characteristics depending on both damping and inertia. Note that the power spectra look different from reported ones (17) because a different parameter is displayed [displacement (here) vs. velocity (17)].

reflecting the larger displacement of the twitching receiver (Fig. 1 A and B). Bimodal, asymmetric probability distributions, indicative of the active origin of spontaneous otoacoustic emissions of vertebrate ears (10) and spontaneous hair-bundle twitches of vertebrate hair cells (13), were observed during self-sustained oscillations (Fig. 1B *Inset*). Such oscillations, however, never occurred in intact live flies ( $n > 80$ ).

Power spectra (Fig. 2) show that the receivers of live and dead flies differ with respect to their fluctuation power and, in addition, to their tuning (Fig. 2A). *In vivo*, the fluctuation power was larger than postmortem (mean  $\langle X^2 \rangle = 36.4 \times 10^{-16}$  vs.  $0.3 \times 10^{-16}$  m<sup>2</sup>), and the natural frequency was lower (mean  $f_0 = 206$  vs. 798 Hz) (Table 1). Notably, the increased fluctuation power

in live flies does not imply that the intact, motile neurons feed energy into the receiver’s fluctuations. First, the lowered natural frequency found in live flies points to a drop in the receiver’s stiffness. Even if this stiffness reduction was achieved purely passively, i.e., without the investment of biological energy, it would increase the receiver’s susceptibility to thermal bombardment and, thus, the fluctuation power. Hence, the rise in fluctuation power observed in live flies may simply reflect a passive stiffness drop. Second, if part of the increase in power should nonetheless be achieved actively, i.e., involve the expenditure of biological energy, the source of energy may not be the neurons. Because live and dead flies are compared, nonneural energy sources such as muscles may be involved. Hence, to assess whether the neurons contribute energy to the receiver’s fluctuations, active alterations of the receiver’s mechanics need to be separated from passive stiffness effects, and neural and nonneural energy contributions need to be distinguished.

We have performed this analysis in four main steps. First, we established the relation between the receiver’s stiffness and its natural frequency for the passive auditory system of dead WT flies. This relation predicts the influence of passive stiffness changes on the receiver’s fluctuations, allowing the separation of the active mechanical effects from passive ones. Second, this prediction was tested by using live mechanosensory mutants with defective mechanosensory neurons. Quantifying the impact of nonneural energy sources on the receiver’s fluctuations, this step allows distinguishing between neural energy contributions and nonneural ones. Third, by using WT and control flies with intact mechanosensory neurons, we assessed the mechanical energy the neurons contribute to the receiver’s fluctuations in healthy live flies. Fourth, by analyzing self-sustained oscillations of the receiver in WT flies, we estimated the energy the neurons are, in principle, able to provide. In a final step, we additionally evaluated the relation between the receiver’s energy and damping to test whether the neurons actively compensate for frictional losses in the auditory system of the fly.

#### Formulating the Prediction: Receiver Fluctuations in Dead WT Flies.

When in equilibrium with its surroundings, a harmonic oscillator such as the fly’s antennal receiver fluctuates in response to thermal noise. These thermal fluctuations obey the equipartition theorem,

$$\frac{1}{2} K \langle X^2 \rangle = \frac{1}{2} k_B T, \text{ with } K = K_S, \quad [3]$$

where  $K$  denotes the effective stiffness of the oscillator,  $K_S$  is its spring constant,  $k_B$  is the Boltzmann constant ( $1.38 \times 10^{-23}$  J/K), and  $T$  is the absolute temperature (293–297 K). The fluctuation power can thus be used to calibrate the effective stiffness of the oscillator,  $K = k_B T / \langle X^2 \rangle$  (23). Notably, at thermal equilibrium only, the effective stiffness revealed by this calibration,  $K$ , represents the intrinsic stiffness of the oscillator, its spring constant,  $K_S$ . If the oscillator is actively held away from equilibrium by a force, however, the calibration yields an effective stiffness that is lower than the spring constant, with the difference reflecting the increase in fluctuation power (and energy) caused by the action of the force. Hence, the two conditions,  $K = K_S$  and  $K < K_S$ , define whether the oscillator satisfies and violates the equipartition theorem, respectively, i.e., whether the oscillator is at thermal equilibrium with its environment ( $K = K_S$ ), or not ( $K < K_S$ ). In either case, the oscillator’s thermal energy is  $k_B T = K \langle X^2 \rangle$ , whereas its mean total energy,  $E$ , i.e., the sum of both thermal and putative, active energy contributions, is  $E = K_S \langle X^2 \rangle$ . This mean total energy of the oscillator can thus be written as

**Table 1. Receiver mechanics**

Strain	$f_0$ , Hz	$\langle X^2 \rangle$ , $10^{-16}$ m <sup>2</sup>	$K$ , $\mu$ N/m	$K_S$ , $\mu$ N/m	$E$ , $k_B T$	$\Delta E$		$\gamma$ , nNm <sup>-1</sup> ·s
						$k_B T$	zJ	
WT dead	798 ± 73	0.3 ± 0.1	131.7 ± 28.5	132.4 ± 24.3	1.0 ± 0.1	0.0	0.1 ± 0.6	28.4 ± 4.6
<i>tilB</i> <sup>2</sup>	766 ± 21	0.4 ± 0.1	118.0 ± 18.0	121.2 ± 6.4	1.0 ± 0.1	0.0	0.2 ± 0.6	25.6 ± 4.4
<i>btv</i> <sup>SP1</sup>	528 ± 24	0.7 ± 0.1	61.1 ± 8.0	57.7 ± 5.4	1.0 ± 0.2	0.0	-0.2 ± 0.6	18.6 ± 3.2*
<i>nompA</i> <sup>2</sup>	406 ± 25	1.2 ± 0.1	34.7 ± 4.1	34.2 ± 4.2	1.0 ± 0.1	0.0	-0.1 ± 0.6	14.7 ± 2.9*
Control <i>tilB</i> <sup>2</sup>	306 ± 45	10.1 ± 5.4	5.0 ± 2.1	19.7 ± 5.8*	4.3 ± 1.1*	3.3*	13.4 ± 4.4*	2.3 ± 0.7*
Control <i>nompA</i> <sup>2</sup>	289 ± 40	10.4 ± 5.4	4.8 ± 2.0	17.6 ± 4.7*	4.0 ± 1.1*	3.0*	12.2 ± 4.6*	1.9 ± 0.7*
Control <i>btv</i> <sup>SP1</sup>	254 ± 54	16.9 ± 10.7	3.2 ± 1.6	14.0 ± 5.6*	4.7 ± 1.1*	3.7*	14.9 ± 4.6*	1.1 ± 0.4*
WT live	206 ± 59	36.4 ± 26.5	2.2 ± 1.8	9.4 ± 5.6*	5.6 ± 2.1*	4.6*	18.8 ± 8.6*	1.2 ± 0.7*
WT self-sustained oscillations	165 ± 47	438.6 ± 272.0	0.12 ± 0.06	6.0 ± 3.2*	50.1 ± 14.9*	49.1*	199.8 ± 60.6*	0.01 ± 0.02*

Strains are sorted by descending  $f_0$ .

\*Significant differences ( $P < 0.05$ ) from  $K_S$  ( $K$ ), unity ( $E$ ), zero ( $\Delta E$ ), and the damping constants of dead WT receivers ( $\gamma$ ) [Wilcoxon-matched pair signed rank tests ( $K$ ,  $E$ ,  $\Delta E$ ) and Mann-Whitney  $U$  test ( $\gamma$ ),  $P \leq 0.001$  for all significant cases].  $N = 20$  receivers per strain (same receivers as in Figs. 2 and 3).

$$E = \frac{K_S}{K} \cdot k_B T. \quad [4]$$

Subtracting the thermal energy, i.e., one  $k_B T$ , then yields the energy gain,  $\Delta E$ ,

$$\Delta E = \left( \frac{K_S}{K} - 1 \right) \cdot k_B T, \quad [5]$$

which corresponds to the excess in the oscillator's mean total energy because of the action of forces other than thermal noise. Hence, by comparing the effective stiffness and the spring constant of the oscillator, active energy contributions can be separated from thermal fluctuations.

The spring constant of a harmonic oscillator, in addition to influencing the fluctuation power, affects the natural frequency. With respect to the natural angular frequency of the undamped system, this latter effect follows the relation

$$K_S = m \omega_0^2, \quad [6]$$

whereby the spring constant is proportional to the squared natural frequency,  $K_S \propto f_0^2$ , and the proportionality factor,  $K_S/f_0^2$ , corresponds to  $(2 \times \pi)^2 \times m$ . If this proportionality factor is known, the spring constant of the oscillator can be derived from the natural frequency. We have used dead WT flies to calibrate this factor: the auditory system of dead flies must be passive, so their antennal receivers can be expected to solely fluctuate in response to thermal noise ( $K = K_S$ ). Given a mean fluctuation power of  $0.3 \times 10^{-16}$  m<sup>2</sup> and a natural frequency of 798 Hz (Table 1), we obtain an average effective stiffness, or spring constant, of 132  $\mu$ N/m (Eq. 3) and a proportionality factor,  $K_S/f_0^2$ , of 207 pN·s<sup>2</sup>·m<sup>-1</sup> (Eq. 6), the latter corresponding to an apparent mass of 5.2 ng. Accordingly, the equation

$$K_S = 207 \cdot 10^{-12} \cdot f_0^2 \quad [7]$$

describes the average relation between the spring constant and the natural frequency for the passive receivers of dead WT flies (Fig. 3A). Notably, this equation allows the prediction of the spring constants of the antennal receivers of live flies. These predicted spring constants, and the effective stiffnesses derived from the receivers' fluctuation powers, will be equal,  $K = K_S$ , assuming that first the apparent mass is constant (Eq. 6) and second that no energy sources other than thermal energy exist (Eq. 4).

**Validating the Prediction: Receiver Fluctuations in Live Mechanosensory Mutants.**

To test the validity of the prediction (Eq. 7), we examined the fluctuations of the receiver in live mutants with defective mechanosensory neurons. In *tilB*<sup>2</sup>, *btv*<sup>SP1</sup>, and *nompA*<sup>2</sup> mutants, the mechanosensory neurons that mediate hearing reportedly display distinct, mutant-specific anatomical defects, including aberrations of dendritic cilia (*tilB*<sup>2</sup>, *btv*<sup>SP1</sup>) (24) and the disconnection of the neurons from the antennal receiver (*nompA*<sup>2</sup>) (25). In line with these structural defects, the receivers of the mutants displayed mutant-specific natural frequencies and fluctuation powers (Fig. 2 B–D and Table 1). Notwithstanding these mechanical differences, the receivers of all three mutants obeyed the prediction (Fig. 3B). The effective stiffness derived from the fluctuation power closely resembled the predicted spring constants,  $K \approx K_S$ , yielding mean total energies approximately equal to thermal energy,  $k_B T$  (Eq. 4 and Table 1). Additionally, the proportionality factors,  $K_S/f_0^2$  ( $201 \pm 30$  pN·s<sup>2</sup>·m<sup>-1</sup> for *tilB*<sup>2</sup>,  $220 \pm 34$  pN·s<sup>2</sup>·m<sup>-1</sup> for *btv*<sup>SP1</sup>, and  $211 \pm 29$  pN·s<sup>2</sup>·m<sup>-1</sup> for *nompA*<sup>2</sup>) were not significantly different from that of dead WT flies ( $207 \pm 33$  pN·s<sup>2</sup>·m<sup>-1</sup>,  $P > 0.05$  in all cases, Mann-Whitney  $U$  tests).

The implications of these findings are threefold. First, the prediction (Eq. 7) is valid; it accurately predicts the spring constants of the antennal receivers of live flies for various natural frequencies. Second, in live flies with defective neurons, the fluctuations of the receiver obey the equipartition theorem; they solely represent thermal fluctuations. Accordingly, nonneural biological energy sources such as muscles do not contribute energy to the receiver's fluctuations. Should additional energy contributions occur in flies with intact mechanosensory neurons, this energy can be assigned to the neurons. Third, the assumption that the apparent mass is constant is legitimate. For the mutants, we found average apparent masses of  $5.1 \pm 0.7$  ng (*tilB*<sup>2</sup>),  $5.6 \pm 0.8$  ng (*btv*<sup>SP1</sup>), and  $5.4 \pm 0.7$  ng (*nompA*<sup>2</sup>). None of these figures differs significantly from that determined for dead WT flies ( $5.2 \pm 0.8$  ng,  $P > 0.05$  in all cases, Mann-Whitney  $U$  tests). Even the disconnection of the neurons from the receiver, as found in *nompA*<sup>2</sup> mutants, does not affect the receiver's apparent mass. Unlike the stiffness of the neurons, their mass seems negligible on the level of the receiver's mechanics.

**Violating the Prediction: Receiver Fluctuations in Live WT and Control Flies.**

The receivers of live WT flies and controls displayed low natural frequencies and high fluctuation powers (Fig. 2A). The corresponding effective stiffness was low, with average values ranging between 5.0 and 2.2  $\mu$ N/m (Table 1). These figures are consistently lower than the predicted spring constants (mean  $K_S = 19.7$ – $9.4$   $\mu$ N/m, Table 1), documenting a breakdown in the

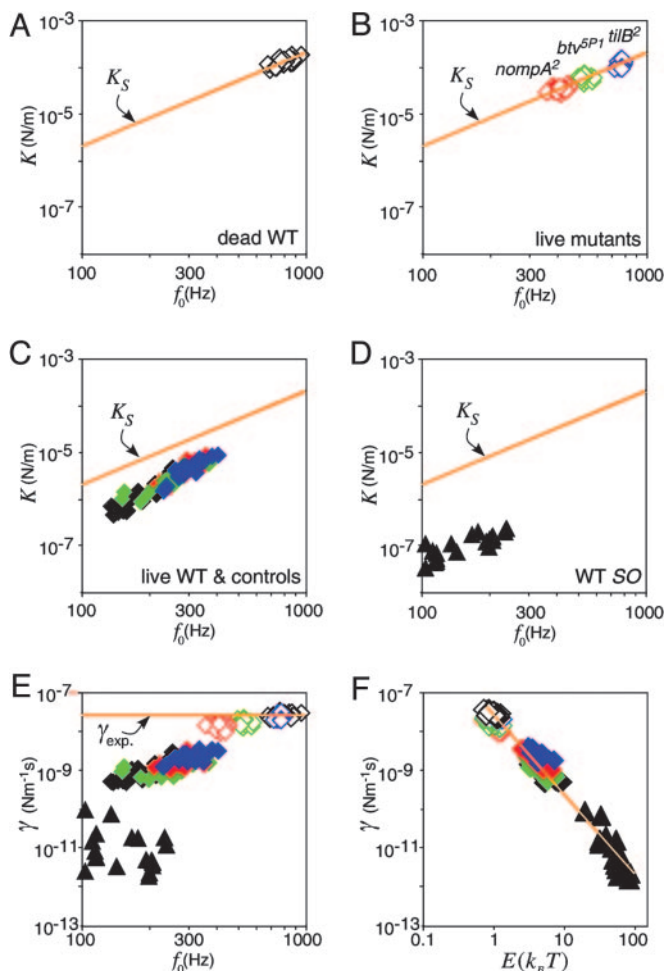


**Fig. 3.** Effective stiffness (A–D) and damping constant (E and F) of the receiver as functions of its natural frequency (A–E) and energy (F) (log-log plots, same receivers as in Fig. 2). (A–D) Effective stiffness in dead WT flies (A), live mechanosensory mutants (B), live WT flies and controls (C), and WT flies displaying self-sustained receiver oscillations (SO) after treatment with DMSO (D,  $\blacktriangle$ ). Color coding is as follows: black, WT flies; blue, *tilB*<sup>2</sup> mutants and controls; green, *btv*<sup>5P1</sup> mutants and controls; and red, *nompA*<sup>2</sup> mutants and controls. Lines show predicted spring constant (Eq. 7). (E and F) Corresponding damping constants plotted against the natural frequency (E) and the mean total energy (F). Symbols and color coding are as in A–D. Lines indicate expected damping constant ( $\gamma_{\text{exp}}$ ) as found in dead WT flies (E) and fitted power function (F). The fit function, which neglects the data of the mutants, is described by  $\gamma = 3 \times 10^{-8} E^{-2}$  ( $r^2 = 0.97$ ,  $P < 0.001$ ).

equipartition theorem ( $K < K_S$ ) (Fig. 3C). Average stiffness ratios,  $K_S/K$ , ranged between 4.0 and 5.6, corresponding to mean total energies,  $E$ , of 4.0–5.6  $k_B T$  (Eq. 4 and Table 1). These figures translate into energy gains,  $\Delta E$ , between 3.0 and 4.6  $k_B T$  or 12–19 zJ (Eq. 5 and Table 1). This additional energy, which is absent in mutants with defective mechanosensory neurons, represents the gain in the receiver's mean total energy caused by energy contributions of the neurons.

#### Excessive Violations: Self-Sustained Oscillations of the Receiver in WT Flies.

To assess the amount of energy the neurons are principally able to contribute to the receiver's fluctuations, we examined self-sustained oscillations of the receivers of WT flies, as measured 15 min after injection of DMSO (Fig. 2E). Under these conditions, the effective stiffness of the receivers was on average 50 times lower than the spring constants expected if the system were passive (0.04 vs. 2.0  $\mu\text{N/m}$ ) (Fig. 3D). This ratio translates

into a mean total energy,  $E$ , of 50  $k_B T$ , corresponding to an energy gain,  $\Delta E$ , of 49  $k_B T$  or 200 zJ (Table 1). These figures represent a rather conservative estimate of the energy gain the neurons exhibit during self-sustained receiver oscillations: the receiver's self-sustained oscillations are not strictly harmonic; the probability distribution is bimodal (Fig. 1B), and frequency spectra display distinct peaks, of which the dominant one was fitted with the model (Fig. 2E). Because it neglects the energy comprised by the other peaks, our analysis is likely to underestimate the total energy of the receiver during self-sustained oscillations.

**Damping Effects.** The sharpness of tuning of a harmonic oscillator is determined by damping. The fluctuations of the fly's antennal receiver are damped by internal friction and viscous interactions with the surrounding air. Provided that this damping is linear and proportional to the velocity of the mass (as is generally assumed for simple harmonic oscillators), the damping constant will not change with the natural frequency and should thus remain unaltered, independent of whether the fly is dead or alive. For the antennal receivers of dead WT flies, we found an average damping constant of 28  $\text{nNm}^{-1}\cdot\text{s}$ . In live flies, the damping constant was significantly reduced (Fig. 3E). The slight, yet significant, reductions observed in *btv*<sup>5P1</sup> and *nompA*<sup>2</sup> mutants (mean values = 19 and 15  $\text{nNm}^{-1}\cdot\text{s}$ , Table 1) are deemed to reflect losses in internal friction caused by the structural aberrations of the neurons (*btv*<sup>5P1</sup>) and the disconnection of the neurons from the receiver (*nompA*<sup>2</sup>). Live WT and control flies lack such structural defects. Nonetheless, the damping constants of their receivers were even lower, ranging between 1 and 2  $\text{nNm}^{-1}\cdot\text{s}$  (Table 1). Moreover, during self-sustained receiver oscillations, the damping constant of WT receivers dropped further down to 0.01  $\text{nNm}^{-1}\cdot\text{s}$ , 2,840 times less than observed after death. Collectively, these pronounced reductions in flies with intact neurons mean that the neurons must provide negative damping and, thus, counteract friction, which implies the expenditure of biological energy. Indeed, our data reveal that the receiver's damping negatively correlates with the fluctuation energy, whereby the damping constant drops inversely with the squared mean total energy of the receiver's fluctuations (Fig. 3F). Such correlation between damping and energy strongly supports the notion that, in *Drosophila*, mechanosensory neurons expend energy to undampen the vibrating structures of the ear.

#### Discussion

An earlier study (17) had shown that the mechanosensory neurons that mediate hearing in *D. melanogaster* are motile and give rise to the mechanical key signatures assigned to the cochlear amplifier in vertebrate ears: the neurons mechanically drive the fly's antennal receiver in the absence of external stimulation and nonlinearly shift its natural frequency with the intensity of sound. This study now documents power gain, the very capacity that defines the cochlear amplifier, for the mechanosensory neurons in the ear of the fly: the neurons are shown to add mechanical energy into the receiver's thermal fluctuations, thus actively amplifying the mechanical input of the ear. This finding validates the concept of the cochlear amplifier for the auditory system of *Drosophila* and shows that, in the fly, this amplifier resides in motile mechanosensory cells. Apparently, the mechanical signatures, the cellular basis, and the characteristic energy budget of the amplifier in the cochlea are copied in the ear of *Drosophila*.

This study identifies two further characteristics of the fly's auditory amplifier that are in accordance with the cochlear amplifier of vertebrates. First, in vertebrates, cochlear amplification is deemed to sharpen the cochlea's mechanical resonances by actively counteracting damping (1–6). In effect, it was this

undamping role that initially gave rise to the concept of the cochlear amplifier, when Gold (2) proposed that an amplificatory process must compensate for frictional losses inside the cochlea to explain the exquisite sensitivity and frequency selectivity of the ear. We show that energy contributions negatively correlate with damping, extending the role of undamping to the auditory amplifier of the fly. Second, in *Drosophila*, amplification appears to operate below maximum capacity; the neurons are able to raise the receiver's mean total energy to at least  $50 k_B T$ , yet energies as little as  $4\text{--}6 k_B T$  are observed in live, healthy flies. This discrepancy is interesting. It suggests that the fly is controlling the amplificatory gain by adjusting the neural energy contribution. If this energy adjustment serves to stabilize the system at the verge of an oscillatory instability, it will maximize the ear's sensitivity to external disturbances imposed by sound (26, 27). Evidence suggests that vertebrate hair cells and also the cochlear mechanics operate near such a critical point, a Hopf

bifurcation (13, 26–29), and the fly's auditory neurons and mechanics may do so as well. By linking nonlinearities, noisy twitches, self-sustained oscillations, and undamping in a mechanistic way (26–28), such critical adjustment of amplification and the underlying concept of self-tuned criticality (27) might explain the vast biophysical parallels between the ears of vertebrates and flies, which, along with multiple molecular parallels (e.g., refs. 19 and 30–33), recommend *Drosophila* for the study of hearing.

We thank Dr. D. F. Eberl (University of Iowa, Iowa City) for *btlv<sup>5P1</sup>* and *tilB<sup>2</sup>* mutants and backgrounds, Dr. M. J. Kernan (Stony Brook University, Stony Brook, NY) for *nompA<sup>2</sup>* mutants and background, and Dr. F. Jülicher for stimulating discussions and critical reading of the manuscript. This work was supported by a Fellowship of the Royal Commission for the Exhibition of 1851 (A.D.L.H.), the University of Bristol (D.R.), Deutsche Forschungsgemeinschaft Grant HBFG-1111-582 (to M.C.G.), and Volkswagen Foundation Grant I/79 147 (to M.C.G.).

- Robles, L. & Ruggero, M. A. (2001) *Phys. Rev.* **81**, 1305–1352.
- Gold, T. (1949) *Proc. R. Soc. London Ser. B* **135**, 492–498.
- Dallos, P. (1996) in *The Cochlea*, eds. Dallos, P., Popper, A. N. & Fay, R. R. (Springer, New York), pp. 1–43.
- Nobili, R., Mammano, F. & Ashmore, J. (1998) *Trends Neurosci.* **21**, 159–167.
- Brownell, W. E., Spector, A. A., Raphael, R. M. & Popel, A. S. (2001) *Annu. Rev. Biomed. Eng.* **3**, 69–104.
- Hudspeth, A. J. (1997) *Curr. Opin. Neurobiol.* **7**, 480–486.
- Bozovic, D. & Hudspeth, A. J. (2003) *Proc. Natl. Acad. Sci. USA* **100**, 958–963.
- Probst, R. (1990) *Adv. Otorhino-laryngol.* **44**, 1–91.
- Köppl, C. (1995) in *Advances in Hearing Research*, eds. Manley, G. A., Klump, G. M., Köppl, C., Fastl, H. & Oeckinghaus, H. (World Scientific, Singapore), pp. 201–216.
- Bialek, W. & Wit, H. P. (1984) *Phys. Lett. A* **104**, 173–178.
- Diependaal, R. J., DeBoer, E. & Viergever, M. A. (1987) *J. Acoust. Soc. Am.* **82**, 917–926.
- Bialek, W. (1987) *Annu. Rev. Biophys. Biophys. Chem.* **16**, 455–478.
- Martin, P., Hudspeth, A. J. & Jülicher, F. (2001) *Proc. Natl. Acad. Sci. USA* **98**, 14380–14385.
- Crawford, A. C. & Fettiplace, R. (1985) *J. Physiol. (London)* **364**, 359–379.
- Göpfert, M. C. & Robert, D. (2001) *Nature* **411**, 908.
- Göpfert, M. C. & Robert, D. (2002) *J. Exp. Biol.* **205**, 1199–1208.
- Göpfert, M. C. & Robert, D. (2003) *Proc. Natl. Acad. Sci. USA* **100**, 5514–5519.
- Kernan, M. & Zuker, C. (1995) *Curr. Opin. Neurobiol.* **5**, 443–448.
- Caldwell, J. C. & Eberl, D. F. (2002) *J. Neurobiol.* **53**, 172–189.
- Kernan, M. J., Cowan, D. & Zuker, C. (1995) *Neuron* **12**, 1105–1206.
- Eberl, D. F., Duyk, G. M. & Perimon, N. (1997) *Proc. Natl. Acad. Sci. USA* **94**, 14837–14842.
- Göpfert, M. C. & Robert, D. (2001) *Proc. R. Soc. London Ser. B* **268**, 333–339.
- Hutter, J. L. & Bechhoefer, J. (1993) *Rev. Sci. Instrum.* **64**, 1868–1873.
- Eberl, D. F., Hardy, R. W. & Kernan, M. J. (2000) *J. Neurosci.* **20**, 5981–5988.
- Chung, Y. D., Zhu, J., Han, Y.-G. & Kernan, M. (2001) *Neuron* **29**, 415–428.
- Eguíluz, V. M., Ospeck, M., Choe, Y., Hudspeth, A. J. & Magnasco, M. O. (2000) *Phys. Rev. Lett.* **84**, 5232–5235.
- Camalet, S., Duke, T., Jülicher, F. & Prost, J. (2000) *Proc. Natl. Acad. Sci. USA* **97**, 3183–3188.
- Jülicher, F., Andor, D. & Duke, T. (2001) *Proc. Natl. Acad. Sci. USA* **98**, 9080–9085.
- Martin, P. & Hudspeth, A. J. (2001) *Proc. Natl. Acad. Sci. USA* **98**, 14386–14391.
- Hassan, B. A. & Bellen, H. J. (2000) *Genes Dev.* **14**, 1852–1865.
- Gillespie, P. G. & Walker, R. G. (2001) *Nature* **413**, 194–202.
- Sidi, S., Friedrich, R. W. & Nicolson, T. (2003) *Science* **301**, 96–99.
- Weber, T., Göpfert, M. C., Winter, H., Zimmermann, U., Kohler, H., Meier, A., Hendrich, O., Rohbock, K., Robert, D. & Knipper, M. (2003) *Proc. Natl. Acad. Sci. USA* **100**, 7690–7695.
- FlyBase Consortium (2003) *Nucleic Acids Res.* **31**, 172–175.